



Measurement-based estimation of the spatial gradient of aerosol radiative forcing

Toshihisa Matsui¹ and Roger A. Pielke Sr.¹

Received 6 February 2006; revised 21 March 2006; accepted 5 May 2006; published 13 June 2006.

[1] This paper diagnoses the spatial mean and the spatial gradient of the aerosol radiative forcing in comparison with those of well-mixed green-house gases (GHG). Unlike GHG, aerosols have much greater spatial heterogeneity in their radiative forcing. The heterogeneous diabatic heating can modulate the gradient in horizontal pressure field and atmospheric circulations, thus altering the regional climate. For this, we diagnose the *Normalized Gradient of Radiative Forcing (NGoRF)*, as a fraction of the present global heterogeneous insolation attributed to human activity. Although the GHG has a larger forcing ($+1.7 \text{ Wm}^{-2}$) as measured than those of aerosol direct (-1.59 Wm^{-2}) and possible indirect effect (-1.38 Wm^{-2}) in terms of a spatially averaged top-of-atmosphere value, the aerosol direct and indirect effects have far greater *NGoRF* values (~ 0.18) than that of GHG (~ 0.003). **Citation:** Matsui, T., and R. A. Pielke (2006), Measurement-based estimation of the spatial gradient of aerosol radiative forcing, *Geophys. Res. Lett.*, 33, L11813, doi:10.1029/2006GL025974.

1. Introduction

[2] Aerosol radiative forcing (ARF) is one of the largest uncertainties with respect to anthropogenic forcing on the present climate system [*National Research Council (NRC)*, 2005]. ARF is composed of direct radiative forcing (ADRF: direct scattering/absorbing of radiation) and indirect radiative forcing (AIRF: scattering/absorbing of radiation due to the modulation of cloud properties by serving as cloud condensation nuclei or ice nuclei).

[3] Advanced satellite instruments can distinguish the small- (submicron) and coarse-mode (supermicron) aerosol optical depths that can be used to estimate the anthropogenic component of aerosol optical depth (AOD) and radiative forcing [*Kaufman et al.*, 2005a]. Combined use of satellite data and chemical-transportation models is also a practical method to estimate ADRF [*Yu et al.*, 2004]. A variety of measurement-based estimations of ADRF is reviewed in *Yu et al.* [2005].

[4] The difficulty of estimating AIRF is linked to the intrinsic complexity of cloud dynamics and microphysics processes. Satellite instruments can measure the relationship between clouds and ambient aerosols on the large scale, and the AIRF can be possibly estimated from the measured correlation. However, a satellite-based estimation has certain limitations. First, it is difficult to distinguish the cloud-

aerosol correlation from a variety of thermodynamic effects on clouds [*Sekigushi et al.*, 2003], although it is possible to reduce such effects by measuring the aerosol-cloud relationship in specific meteorological conditions [*Koren et al.*, 2004; *Matsui et al.*, 2006]. Second, the measured aerosol-cloud correlation does not imply physical causality; i.e., it is uncertain whether aerosols affect clouds (via nucleation or the semi-direct effect) or clouds affect aerosols (via wet deposition) [*Kaufman et al.*, 2005b].

[5] The ARF is typically discussed and compared as a global-scale spatial mean top-of-atmosphere (TOA) radiative forcing. Unlike greenhouse gases (GHG), however, aerosols have a much greater heterogeneity of their radiative forcing in time and space. This forcing can modulate mesoscale and large-scale circulations, which have potential impacts on the regional climate through dynamical feedback [*Menon et al.*, 2002; *Lau et al.*, 2006; *Takemura et al.*, 2005]. The spatial mean TOA radiative forcing may be ineffective in representing such effects [*NRC*, 2005].

[6] This paper evaluates the mean and spatial gradient of aerosol radiative forcing in comparison with that of the well-mixed GHG. The appropriate metric to assess the importance of the gradient of diabatic heating is the resulting gradients in the horizontal pressure field that fundamentally drives the atmospheric circulation [*Gill*, 1982]. We emphasize that this study does not aim to compare methods or assess the detailed uncertainties in estimating the global mean ARF among different studies.

2. Methodology

[7] The estimation of ARF in this paper is limited to the shortwave radiation and over tropical oceans between 37°N to 37°S for the period starting from 1st March 2000 to 28th February 2001, since i) the energy budget in the tropics is a critical factor for the global atmospheric circulation; and ii) the cloud and aerosol properties were compiled in this period and correspond to the domain in our previous study [*Matsui et al.*, 2006]. The atmospheric radiative transfer was computed by the NASA Langley-version of the Fu-Liou code, which updated several components of the original four-stream correlated-k radiative transfer code [*Fu and Liou*, 1993] (Charlock and Rose, personal communication, 2005). The vertical profile of atmospheric temperature, water vapor mixing ratio, and ozone mixing ratio are derived from the climatological values of sounding [*McClatchey et al.*, 1972]. The spectral ocean surface albedo is computed from an empirical look-up table [*Jin et al.*, 2004].

[8] ADRF is estimated from the difference in the shortwave radiative heating rate between the current AOD and the potential AOD in clear sky conditions. The current AOD is obtained by the Moderate Resolution Imaging Spectro-

¹Department of Atmospheric Science, Colorado State University, Ft. Collins, Colorado, USA.

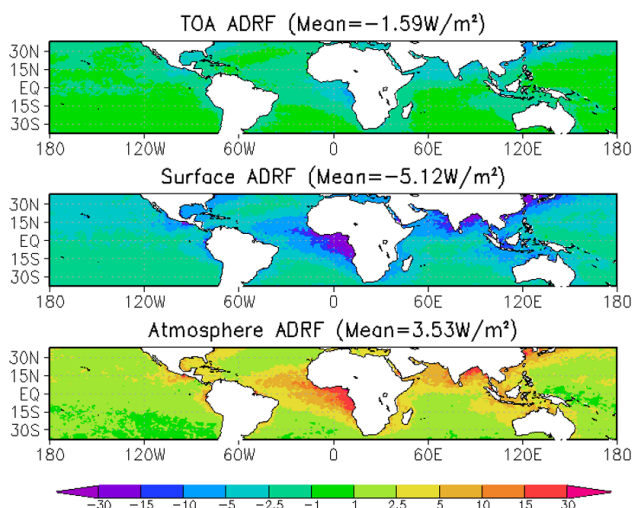


Figure 1. Shortwave aerosol direct radiative forcing (ADRF) for top-of atmosphere (TOA), surface, and atmosphere.

radiometer (Terra MODIS) Level-3 (collection 4) instantaneous AOD at $0.55 \mu\text{m}$ and $0.865 \mu\text{m}$, which are archived on a global $1^\circ \times 1^\circ$ latitude-longitude grid. Total column AOD is subdivided into dust, sea salt, organic carbon, black carbon and sulfate components for each vertical atmospheric layer based on the co-located daily product of the chemical transportation model [Chin *et al.*, 2004]. Potential AOD is estimated from the sum of estimated sea salt and dust AOD, although the potential AOD can be also estimated from the small-mode fraction of MODIS AOD [Kaufman *et al.*, 2005a]. Aerosol optical properties are based on the Optical Properties of Aerosol and Cloud (OPAC) values [Hess *et al.*, 1998].

[9] Matsui *et al.* [2006] found relationships between marine low cloud properties, ambient thermodynamics and aerosols. For AIRF, potential low cloud properties (column cloud effective radius, liquid water path, and cloud fraction) are estimated as a function of ambient aerosol index (AI: AOD multiplied by the Ångström exponent) as well as lower-tropospheric stability (LTS: potential temperature difference between the atmosphere at the 700 mb level and the surface), by using the correlation given by Matsui *et al.* [2006]. The estimation of AIRF accounts for low liquid clouds with cloud top temperatures greater than 273 K. The approach is to perturb the observed *current* cloud properties for the *potential* cloud properties by using the empirical relationship between the ambient AI and cloud properties for a given LTS. Although this method helps to resolve the effect of aerosols and thermodynamics on cloud properties to some degree, physical causality is still uncertain. Thus, the estimated radiative forcing could be interpreted as the *possible* AIRF. The current and potential AIs are derived from the identical AOD to those used in the estimation of ADRF. The ADRF is not included in the estimation of AIRF.

3. Results

3.1. Aerosol Direct Radiative Forcing (ADRF)

[10] Figure 1 shows the annually averaged ADRF over tropical oceans. The mean values of ADRF for our study

area (37°S to 37°N) are -1.59 and -5.12 Wm^{-2} at the TOA and the surface level. The large gap between the TOA and surface ADRF is explained by the strong atmospheric heating rate (3.53 Wm^{-2}) due to presence of absorbing aerosols. These values are slightly higher than those given by Yu *et al.* [2004], since this study focuses on tropical oceans where annual incoming solar radiation is high. The ADRF is quite heterogeneous in space, ranging from 0 to -30 Wm^{-2} at the surface level. Large ADRF at the surface and in the atmosphere exists off the west coast of Africa and the coastal zone along the South to East Asia. Although different assumptions of single scattering albedo of absorbing aerosols could change the mean radiative forcing [Yu *et al.*, 2004], it does not change the annual spatial pattern of ADRF to a great extent.

[11] Figure 2 shows the vertical profile of atmospheric heating rate due to shortwave ADRF at latitudes of 35°N , 15°N , and 5°S . At the latitude of 35°N , there is weak boundary layer heating off the east coast of U.S. and across the Mediterranean Sea. The largest heating appears off the east coast of China, with the heating concentrated in the lower atmospheric layer. At the latitude of 15°N , strong boundary layer heating exists off the west coast of the Yucatan Peninsula due to the smoke emitted from biomass burning, and the strong peak over the Bay of Bengal is due to a relatively high concentration of soot [Ramanathan *et al.*, 2001]. This South Asian brown haze induces atmospheric heating up to 0.5 K day^{-1} (about 20 Wm^{-2}) in the bottom atmospheric layer. Menon *et al.* [2002] showed that the presence of the ADRF of black carbon modulates the general circulation and static stability fields elsewhere in the globe. Lau *et al.* [2006] found that ADRF over Tibetan Plateau can modulate the Asian Monsoon through the “elevated heat pumping” mechanism. At the latitude of 5°S , strong atmospheric heating extends up to the 600 mb pressure level off the west coast of Africa, where biomass burning frequently occurs due to agricultural practices. These vertical profiles and magnitudes of heating could be different for different seasons comparatively, and they must have unrevealed, dynamical interactions between the ADRF and regional climate.

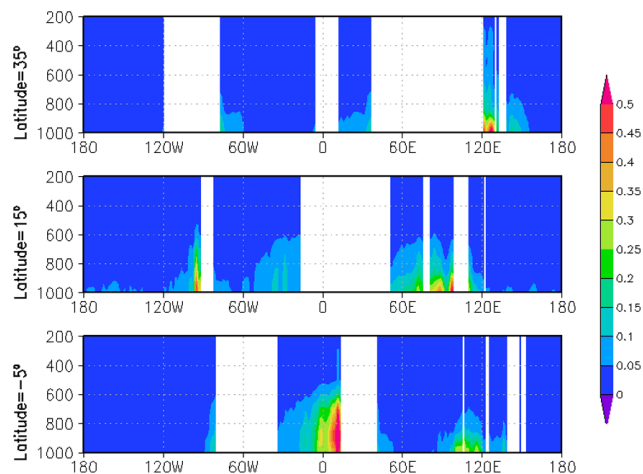


Figure 2. Vertical profile of atmospheric heating rate (K day^{-1}) due to shortwave ADRF. Vertical coordinate is pressure level (mb).

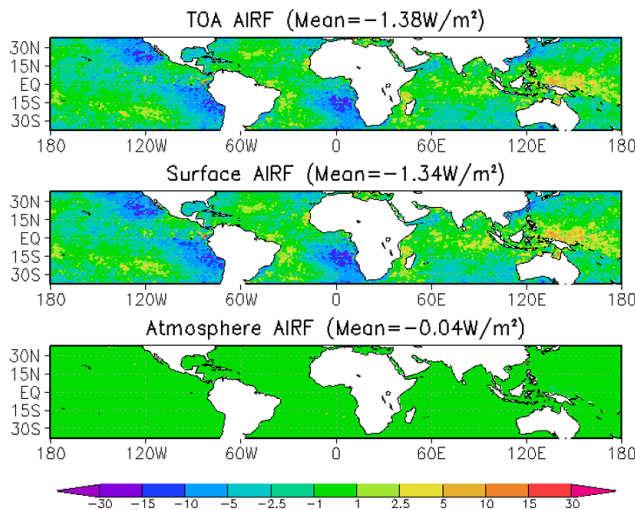


Figure 3. Shortwave aerosol indirect radiative forcing (AIRF) for top-of atmosphere (TOA), surface, and atmosphere.

3.2. Aerosol Indirect Radiative Forcing (AIRF)

[12] Figure 3 shows the shortwave AIRF over the tropical ocean. The domain averaged AIRF is -1.38 Wm^{-2} at the TOA level. It is slightly higher than the estimate (-0.6 to -1.2 Wm^{-2}) given by *Sekiguchi et al.* [2003]. The estimated AIRF is also heterogeneous in space, ranging from 0 to -30 Wm^{-2} at the surface level. The strongest AIRF exists off the west coast of California, Chile, and Namibia, where strong temperature inversions (high LTS) exist. Over the Atlantic Ocean, the spatial pattern of AIRF reasonably agrees to the result given by *Kaufman et al.* [2005b]. In high LTS regions, the measured correlation by *Matsui et al.* [2006] tends to increase the cloud fraction for high AI, which strongly contributed to the large values of AIRF. *Sekiguchi et al.* [2003] also show that large AIRF exist over the downwind of continents. The peak ADRF regions appear to be associated with very weak or positive AIRF, possibly because the high ADRF enhances the evaporation of low clouds [*Koren et al.*, 2004]. The estimation of AIRF could be significantly different, in terms of the spatial mean and the spatial pattern, if cold cloud-aerosol interaction is included (J. C. Lin et al., Effects of biomass burning-derived aerosols on precipitation and clouds in the Amazon Basin: A satellite-based empirical study, submitted to *J. Geophys. Res.*, 2006).

4. Spatial Mean Radiative Forcing

[13] Anthropogenic radiative forcing is currently expressed as the spatial (often on global scale) mean TOA radiative forcing in climate assessment reports or journals. This metric is useful for the energy budget of the entire Earth as a closed system, and for intercomparison among different studies and different forcing.

[14] Figure 4 compares the tropical-ocean averaged radiative forcing between the GHG effect, aerosol direct effect, and aerosol indirect effect. GHG radiative forcing (GRF) was estimated from the difference in infrared radiative cooling between pre-industrial and current levels of CO_2

(285.43 and 336.77 ppmv), N_2O (0.28 and 0.32 ppmv), CH_4 (0.86 and 1.79 ppmv), CFC-11 (0.0 and $268. \times 10^{-6}$ ppmv), CFC-12 (0.0 and $503. \times 10^{-6}$ ppmv), and CFC-113 (0.0 and $105. \times 10^{-6}$ ppmv), respectively. We should note again that shortwave ADRF is estimated in the clear sky, and shortwave AIRF is estimated without ADRF. Therefore, i) total ARF is not equivalent to the sum of ADRF and AIRF; ii) ADRF and AIRF could be overestimated by neglecting cold clouds in the tropics.

[15] In the spatial mean radiative forcing, GHG has the largest positive forcing ($+1.7 \text{ Wm}^{-2}$), and aerosols appear to have an equivalent negative forcing (-1.59 and -1.38 Wm^{-2}) (Figure 4). However, this comparison may not be useful to discuss the effect on the climate, because the global climate is suitably described as a combination of regional climates. Heterogeneous radiative forcing potentially induces a much greater impact on the regional climate by modulating atmospheric circulations [*Menon et al.*, 2002; *Lau et al.*, 2006] and ocean circulation [*Takemura et al.*, 2004].

5. Spatial Gradient of Radiative Forcing

[16] In order to account for radiative forcing on the atmospheric motion, we derive the spatial gradient of radiative forcing (*GoRF*). This is because fluid motion works to reduce the temperature gradient given by the heterogeneous insolation, as influenced by the Earth's rotation, friction, and other dynamical processes [*Gill*, 1982]. The types of circulation depend on the horizontal and vertical scale of the gradient and the latitude, ranging from mesoscale to planetary-scale circulations; thus, the gradient was computed for different spatial scales (e.g., in this study, horizontal distance from 1° to 20°). In addition, we normalize the anthropogenic component of *GoRF* with respect to the total component of *GoRF* for each spatial scale. The derived normalized gradient of radiative forcing (*NGoRF*) essentially means the fraction of the present Earth's heterogeneous insolation attributed to human activity on different horizontal scales. *NGoRF* for the meridional component is mathematically represented as

$$NGoRF = \frac{GoRF_{anthro}}{GoRF_{total}}$$

where

$$GoRF_{total} = \frac{\partial R_{total}}{\partial \lambda}$$

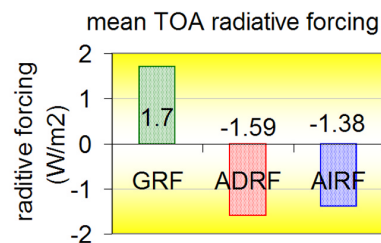


Figure 4. Comparison of Mean TOA radiative forcing between infrared GRF, shortwave ADRF, and shortwave AIRF.

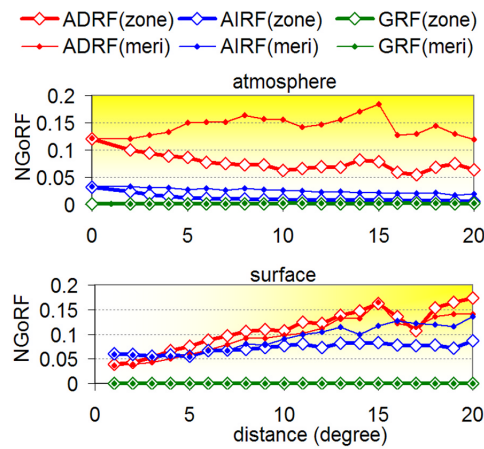


Figure 5. Comparison of the meridional and the zonal component of $NGoRF$ between infrared GRF, shortwave ADRF, and shortwave AIRF for atmosphere and surface.

$$GoRF_{anthro} = \frac{\overline{\partial R_{anthro}}}{\partial \lambda}$$

where $R_{total} = R_{total}(\lambda, \varphi)$ represents the present-time total radiative forcing at the surface level or in the atmosphere, $R_{anthro} = R_{anthro}(\lambda, \varphi)$ represent the anthropogenic component (GRF, ADRF, or AIRF in this study) of radiative forcing, λ represents longitude, φ represents latitude, overbar means the spatial averaging. The zonal component of $NGoRF$ can be described in a similar manner. In this study, R_{total} is limited to the observed (1st March 2000 to 28th February 2001) aerosols, marine low cloud, GHGs, and sea surface temperature. For this, we 1) derived the total and anthropogenic component of $GoRF$ for the each neighboring pixels, and averaged over the entire domain to compute the $NGoRF$; and 2) aggregated the R_{total} and R_{anthro} map on different horizontal scales ($\lambda = 1^\circ, 2, \dots, 20^\circ$) to re-do the process 1) for computing the multi-scale $NGoRF$.

[17] Figure 5 shows the multi-scale $NGoRF$ in the atmosphere and at the surface level of shortwave ADRF, shortwave AIRF, and infrared GRF. $NGoRF$ in the atmosphere on the spatial scale of less than a few degrees of latitude/longitude are associated with mesoscale circulations. $NGoRF$ in the atmosphere on larger scales (up to 20°) is associated synoptic features such as the Hadley Circulation or the Walker Circulation in the tropics. Both are associated with meridional and zonal baroclinic atmospheric processes.

[18] Figure 5 shows that ADRF exhibits the highest $NGoRF$ (~ 0.18) for all horizontal scales. This means that the ADRF contributes up to 18% with respect to the meridional gradient of insolation in the current atmosphere. At the surface level, $NGoRF$ on the large horizontal scale would be linked to the ocean insolation patterning. Figure 5 indicates that ADRF and AIRF show large contributions to the current ocean insolation patterning. *Takemura et al.* [2004] showed that the ADRF and AIRF have strong feedbacks to the simulated general circulation, when the global atmospheric model is coupled with the ocean circulation model.

[19] Although the TOA radiative forcing of GRF is the largest (Figure 4), the $NGoRF$ of the GRF is almost negligible (~ 0.003) in comparison with AIRF (~ 0.14) and ADRF (~ 0.18). Our study did not measure the interaction between the homogenous GRF and the heterogeneous ARF and how it affects the general circulation and regional climate. However, basic atmospheric dynamics requires that atmospheric diabatic heating anomalies necessarily result in wind circulation anomalies. Thus, the aerosols have the potential to have a major effect on the weather and climate patterns in regions with a high aerosol gradient.

6. Summary

[20] We present a measurement-based estimation of the spatial gradient of aerosol radiative forcing. The $NGoRF$ is introduced to represent the potential effect of the heterogeneous radiative forcing on the general circulation and regional climate. At present, there is no single metric of radiative forcing that can represent the complex interactions of atmospheric circulation [NRC, 2005]. While the spatially resolved $NGoRF$ could add to the ability to quantify regional climate forcing, we encourage the community to test and develop the $NGoRF$ for different years, seasons, over land, and patterns of sea surface temperature via numerical models or analytic solutions.

[21] **Acknowledgments.** This work is funded by NASA CEAS fellowship, NAG5-12105 and NASA Grant NNG04GB87G. The authors would like to thank T. Charlock and F. Rose at NASA Langley for providing the radiative transfer code packages, and Chris Castro and anonymous reviewers for valuable comments. This paper is dedicated to Yoram J. Kaufman, who inspired this study.

References

- Chin, M., A. Chu, R. Levy, L. Remer, Y. Kaufman, B. Holben, T. Eck, P. Ginoux, and Q. Gao (2004), Aerosol distribution in the Northern Hemisphere during ACE-Asia: Results from global model, satellite observations, and Sun photometer measurements, *J. Geophys. Res.*, *109*, D23S90, doi:10.1029/2004JD004829.
- Fu, Q., and K.-N. Liou (1993), Parameterization of the radiative properties of cirrus clouds, *J. Atmos. Sci.*, *50*, 2008–2025.
- Gill, A. (1982), *Atmosphere-Ocean Dynamics*, 662 pp., Elsevier, New York.
- Hess, M., P. Koepke, and I. Schult (1998), Optical properties of aerosols and clouds: The software package OPAC, *Bull. Am. Meteorol. Soc.*, *79*, 831–844.
- Jin, Z., T. P. Charlock, W. L. Smith Jr., and K. Rutledge (2004), A parameterization of ocean surface albedo, *Geophys. Res. Lett.*, *31*, L22301, doi:10.1029/2004GL021180.
- Kaufman, Y. J., O. Boucher, D. Tanré, M. Chin, L. A. Remer, and T. Takemura (2005a), Aerosol anthropogenic component estimated from satellite data, *Geophys. Res. Lett.*, *32*, L17804, doi:10.1029/2005GL023125.
- Kaufman, Y. J., I. Koren, L. A. Remer, D. Rosenfeld, and Y. Rudich (2005b), The effect of smoke, dust and pollution aerosol on shallow cloud development over the Atlantic Ocean, *Proceedings Natl. Acad. Sci. U.S.A.*, *102*(32), 11,207–11,212.
- Koren, I., Y. J. Kaufman, L. A. Remer, and J. V. Marins (2004), Measurement of the effect of Amazon smoke on inhibition of cloud formation, *Science*, *303*, 1342–1345.
- Lau, K.-M., M.-K. Kim, and K.-M. Kim (2006), Aerosol induced anomalies in the Asian summer monsoon—the role of the Tibetan Plateau, *Clim. Dyn.*, in press.
- Matsui, T., H. Masunaga, S. M. Kreidenweis, R. A. Pielke Sr., W.-K. Tao, M. Chin, and Y. J. Kaufman (2006), Satellite-based assessment of marine low cloud variability associated with aerosols, atmospheric stability, and the diurnal cycle, *J. Geophys. Res.*, doi:10.1029/2005JD006097, in press.
- McClatchey, R. A., W. Fenn, J. E. A. Selby, F. E. Volz, and J. S. Garing (1972), Optical properties of the atmosphere, *Environ. Res. Pap.* *411*, 108 pp., Air Force Cambridge Res. Lab., Cambridge, Mass.
- Menon, S., J. E. Hansen, L. Nazarenko, and Y. Luo (2002), Climate effects of black carbon aerosols in China and India, *Science*, *297*, 2250–2253.

- National Research Council (2005), *Radiative Forcing of Climate Change: Expanding the Concept and Addressing Uncertainties*, National Academies Press, Washington, D. C. (Available at <http://www.nap.edu/openbook/0309095069/html/>).
- Ramanathan, V., P. J. Crutzen, J. T. Kiehl, and D. Rosenfeld (2001), Aerosols, climate, and the hydrological cycle, *Science*, *294*, 2119–2124.
- Sekiguchi, M., T. Nakajima, K. Suzuki, K. Kawamoto, A. Higurashi, D. Rosenfeld, I. Sano, and S. Mukai (2003), A study of the direct and indirect effects of aerosols using global satellite data sets of aerosol and cloud parameters, *J. Geophys. Res.*, *108*(D22), 4699, doi:10.1029/2002JD003359.
- Takemura, T., T. Nozawa, S. Emori, T. Y. Nakajima, and T. Nakajima (2005), Simulation of climate response to aerosol direct and indirect effects with aerosol transport-radiation model, *J. Geophys. Res.*, *110*, D02202, doi:10.1029/2004JD005029.
- Yu, H., R. E. Dickinson, M. Chin, Y. J. Kaufman, M. Zhou, L. Zhou, Y. Tian, O. Dubovik, and B. N. Holben (2004), Direct radiative effect of aerosols as determined from a combination of MODIS retrievals and GOCART simulations, *J. Geophys. Res.*, *109*, D03206, doi:10.1029/2003JD003914.
- Yu, H., et al. (2005), A review of measurement-based assessment of aerosol direct radiative effect and forcing, *Atmos. Chem. Phys. Disc.*, *5*, 7647–7768.

T. Matsui and R. A. Pielke Sr., Department of Atmospheric Science, Colorado State University, Ft. Collins, CO 80523–1371, USA. (matsui@atmos.colostate.edu)